Hindawi Publishing Corporation
Journal of Nanomaterials
Volume 2014, Article ID 430164, 6 pages
http://dx.doi.org/10.1155/2014/430164

Research Article

Investigation of the Optimal Parameters in Hydrothermal Method for the Synthesis of ZnO Nanorods

Ying-Chung Chen,[1] Huan-Yi Cheng,[1] Cheng-Fu Yang,[2] and Yuan-Tai Hsieh[3]

[1] *Department of Electrical Engineering, National Sun Yat-Sen University, Kaohsiung 80424, Taiwan*
[2] *Department of Chemical and Materials Engineering, National University of Kaohsiung, Kaohsiung 81147, Taiwan*
[3] *Department of Electronic Engineering, Southern Taiwan University, Tainan 71005, Taiwan*

Correspondence should be addressed to Cheng-Fu Yang; cfyang@nuk.edu.tw

Received 7 May 2014; Accepted 16 June 2014; Published 25 June 2014

Academic Editor: Teen-Hang Meen

We investigated a two-step method to deposit the ZnO-based nanostructure films, including nanorods and nanoflowers. In the first step, sputtering method was used to deposit the ZnO films on SiO_2/Si substrates as the seed layer. In the second step, $Zn(NO_3)_2$–$6H_2O$ and $C_6H_{12}N_4$ were used as precursors and hydrothermal process was used as the method to synthesize the ZnO films. After that, the ZnO films were measured by an X-ray diffraction pattern and a FESEM to analyze their crystallization and morphology. We had found that the ZnO films had three different morphologies synthesized on ZnO/SiO_2/Si substrates, including irregular-plate structure films, nanorod films, and beautiful chrysanthemum-like clusters (nanoflower films). We would prove that the face direction of ZnO/SiO_2/Si substrates in the hydrothermal bottle and deposition time were two important factors to influence the synthesized results of the ZnO films.

1. Introduction

Transparent conducting oxide (TCO) films based on zinc oxide (ZnO) are promising candidates for applications in various optoelectronic devices. However, ZnO-based films present a lot of advantages such as higher transparency in infrared region and high chemical stability under the hydrogen plasma as compared to tin-doped indium oxide (ITO). For that, transparent conducting ZnO-based films have already been extensively used in solar cells, light-emitting diodes, and liquid crystal displays as a substitute for ITO [1]. ZnO nanorods have attracted much attention of researchers due to their various applications such as solar cells [2], light-emitting diodes [3], and super hydrophobic surfaces [4]. ZnO nanorods are also considered as a promising material of gas sensors because of its high electrochemical stability, nontoxicity, suitability to doping, and low material cost [5]. The sensing characteristics of a sensor depend on the shape and dimensionality of the sensing material a lot, so that multiplicate ZnO nanostructures have been synthesized and studied in the past decade. Those researches have shown that one-dimensional (1D) ZnO nanostructures possess a large surface-to-volume ratio, which can absorb more tested molecules on the surface and have high gas-sensing efficiency [5–7].

Up to now, 1D ZnO-based nanotubes, nanowires, nanorods, and nanotetrapods have been synthesized by various physical and chemical methods and used to fabricate gas sensors. Synthesis of the ZnO nanorods based on vapor phase deposition, such as metal-organic chemical vapor deposition, vapor-liquid-solid reaction, vapor-solid reaction, chemical vapor deposition, and pulsed laser deposition are expensive methods because of the sophisticated equipment or high temperature required [8]. In contrast to the above growth techniques, the aqueous solution growth method can be a simple and cost-effective technique because it has no drawbacks of expensive apparatus, rigorous condition, complex process, low yield, and high temperature needed. Recently, a hydrothermal method has also been developed to fabricate 1D ZnO nanostructures. Jiaqiang et al. had

prepared ZnO nanorods by a hydrothermal process with cetyltrimethyl ammonium bromide and zinc powder at 182°C [9]; Li et al. had synthesized ultralong ZnO nanowires by a hydrothermal reaction of Zn foil and aqueous $Na_2C_2O_4$ solution at 140°C [6]; Kim and Yong had synthesized ZnO nanorod-bundle powders by a hydrothermal reaction using zinc chloride and ammonium hydroxide solution at 150°C [7]. Those results prove that the hydrothermal method provides a convenient and low cost route for the construction of rod- or wire-typed ZnO nanostructures. Herein, we used SiO_2/Si as substrates and investigated a two-step method to find a simple process for growing ZnO-based nanorods. In the first step, the ZnO seed layer was deposited using sputter method. In the second step, we used $Zn(NO_3)_2$–$6H_2O$ and $C_6H_{12}N_4$ (Hexamethylenetetramine, HMTA) as precursors to develop a low-temperature hydrothermal route (at 100°C) for synthesizing the nanorod-typed ZnO nanostructures. We would show that faces' direction of ZnO/SiO_2/Si substrates in the hydrothermal bottle and deposition time were two important factors to grow the ZnO nanorods.

2. Experimental

ZnO powder was mixed with polyvinylalcohol (PVA) as binder, and then the mixed powder was uniaxially pressed into pellets of 5 mm thickness and 54 mm diameter using a steel die. After debindering, the ZnO pellets were sintered at 1200°C for 2 h. SiO_2/Si substrates with an area of 2 × 2 cm^2 were cleaned ultrasonically with isopropyl alcohol (IPA) and deionized (DI) water and then dried under a blown nitrogen gas. Our growth procedure for ZnO-based nanostructures consisted of two steps. At the first step, ZnO targets were used to deposit ZnO films with a thickness of ~300 nm by sputtering deposition technique to form the ZnO/SiO_2/Si substrates. ZnO films were subsequently used as seed layer for the growth of ZnO nanostructures. The deposition parameters for seed layer were RF power of 85 W, working pressure of 15 × 10^{-3} Torr in pure Ar (99.99%) ambient, deposition at room temperature (RT), and the deposition time of 30 min, respectively. In the second step, ZnO nanostructures were grown on seed-deposition ZnO/SiO_2/Si substrates from an equimolar aqueous solution of $Zn(NO_3)_2$–$6H_2O$ (99.9% purity) and $C_6H_{12}N_4$ (99.9% purity, Hexamethylenetetramine, HMTA) in deionized water [10–12]. In order to fabricate ZnO nanorods, $Zn(NO_3)_2$–$6H_2O$ and $C_6H_{12}N_4$ were used as reagents, the diluted solution with concentration of 0.1 M in DI water, and volume of DI water was 20 g. After mixing at 65°C for 40 min the diluted solution was put into a bottle and the ZnO nanostructures were synthesized on the seed ZnO/SiO_2/Si layer by using hydrothermal process at 100°C for 1 h, 3 h, and 5 h, respectively. The sketch of the experimental set for growing ZnO nanostructure films was shown in Figure 1, two different directions were compared in this study, and ZnO films were deposited on both up and down faces of ZnO/SiO_2/Si substrates. Surface morphology of ZnO films was observed using a field emission scanning electron microscopy (FESEM), and their crystalline structures were measured using X-ray diffraction (XRD) patterns with Cu Kα radiation (λ = 1.5418 Å).

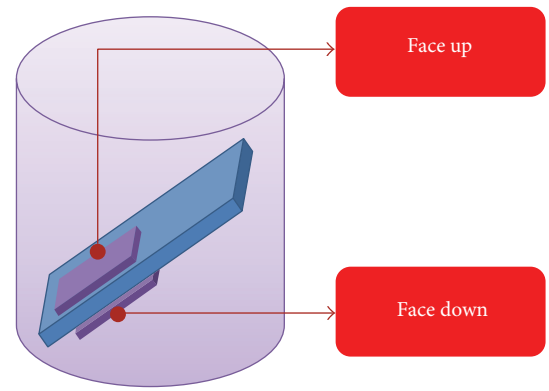

Figure 1: Structure for growing nanostructure ZnO films.

3. Results and Discussion

To investigate the general morphologies of hydrothermal-deposited ZnO nanostructures, the synthesized products are first examined by FESEM and demonstrated in Figure 2 under lower magnifications. The hydrothermal process is based on the formation of solid phase from a solution, which involves two steps as nucleation and growth [12]. At first in the nucleation process, the clusters of molecules formed undergo rapid decomposition ($Zn(NO_3)_2$–$6H_2O$ is used as source) and particles combine to grow up on the substrate surface of the ZnO seed layer by nonheterogeneous reactions. Figure 2(a) shows the down-face morphology of the 1 h deposited ZnO films; there are no nanorods or nanoflowers that appeared on the ZnO/SiO_2/Si substrates in the first 1 h growth and only irregular-plate structure films were observed, which was identical to the up-face morphology. In the past, Liu et al. explained that the different morphology of the deposited ZnO films on different substrates should be related to the lattice structure and defects on the substrates' surfaces, which were key factors for chemical adsorption and subsequent nucleation and growth [12]. However, we will show that the deposition time and the face of substrates are two important factors to synthesize the ZnO nanorods on ZnO/SiO_2/Si substrates.

From the obtained FESEM observations in Figure 2(b), it is confirmed that as deposition time was 3 h, the synthesized products were only ZnO nanorods with a diameter ranging from 65 to 200 nm, grown in very large quantity, and the irregular-plate structure shown in Figure 2(a) was not observed. As the ZnO nanorods are synthesized in large quantity and densely populated, hence it is seen that many nanorods are not joined with each other at each side of the nanorods, which suggests that the ZnO nanorods can have enough space to detect gas and act as a sensor. When deposition time was increased to 5 h, as Figure 2(c) shows, the synthesized products were not only nanorods, but also beautiful chrysanthemum- (flower-) like clusters grown above the nanorods in very large quantity. The flower-like

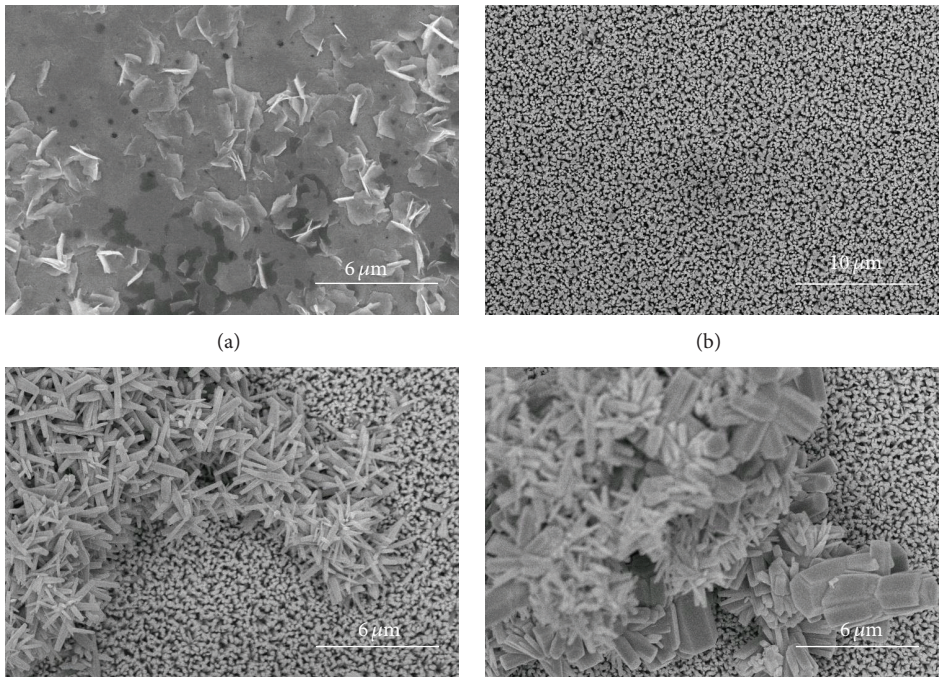

Figure 2: Surface morphologies of the deposited ZnO films synthesized at different faces and time and under different magnifications. Down face (a) 1 h, (b) 3 h, and (c) 5 h; up face (d) 5 h, respectively.

microstructures also consist of nanorods with a diameter ranging from 200 to 350 nm and length of 1.5–3 μm, and the flower-like architectures become dominant with substrate coverage of about 50%. However, as the surface morphology in up face was observed, as Figure 2(d) shows, the size of the flower-like nanostructures was not uniform, while a few of the large rods with different diameters and lengths were also present. The flower-like and large-rod architectures developed further and became dominant with substrate coverage of about 80%. Those results suggest that the ZnO deposition rate of up-face substrates is quicker than that of down-face substrates and 3 h is the optimal time to grow the ZnO nanorods as the gas sensors.

The XRD results in Figure 3 reveal that all the ZnO-deposited films were of hexagonal wurtzite structure, and the three patterns of the ZnO-deposited films were in agreement with but different from the diffraction data from standard card (JCPDS 36-1451). The mainly crystalline peak of ZnO in JCPDS 36-1451 is (101), which is located around 2θ~36.25°. By comparison, the stronger intensity of (002) diffraction peak was found in Figure 3 for all deposited ZnO films, suggesting that all the films exist in high *c*-axis orientation. Accordingly, the tendency of c-orientation (200) peak was increased as the deposition time increased from 1 h to 3 h. The increase of the full width at half maximum (FWHM) values of (200) peak indicates that the crystallization of ZnO films increases as the synthesized time increases.

Results in Figure 3 indicate that 1 h deposited ZnO films had a (002) peak and two weak (100) and (110) peaks; 3 h deposited ZnO films only had a strong (002) peak; and 5 h deposited ZnO films had a strong (002) peak and two weak (100) and (110) peaks. The (002), (100), and (110) peaks are preferred orientation with the *c*-axis perpendicular to the substrate. Those results illustrate that the diffraction data on the surface match the morphology as well as crystal orientation of the resultant films. An energy dispersive spectroscopic (EDS) analysis of the ZnO films in Figure 4 (up-face and deposition time was 3 h) shows that the products were composed mainly of Zn and O elements, consistent with

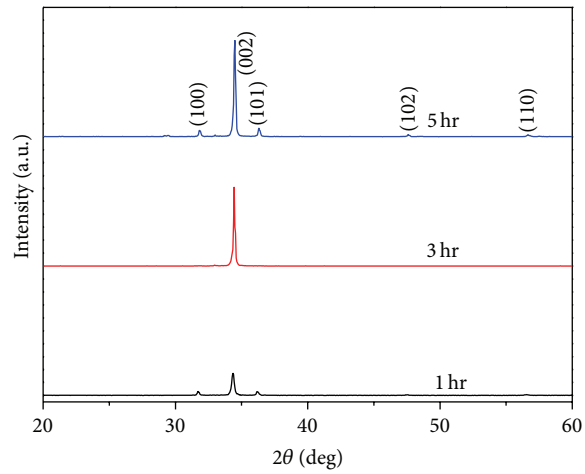

Figure 3: XRD patterns of the down-face ZnO films synthesized at different deposition time.

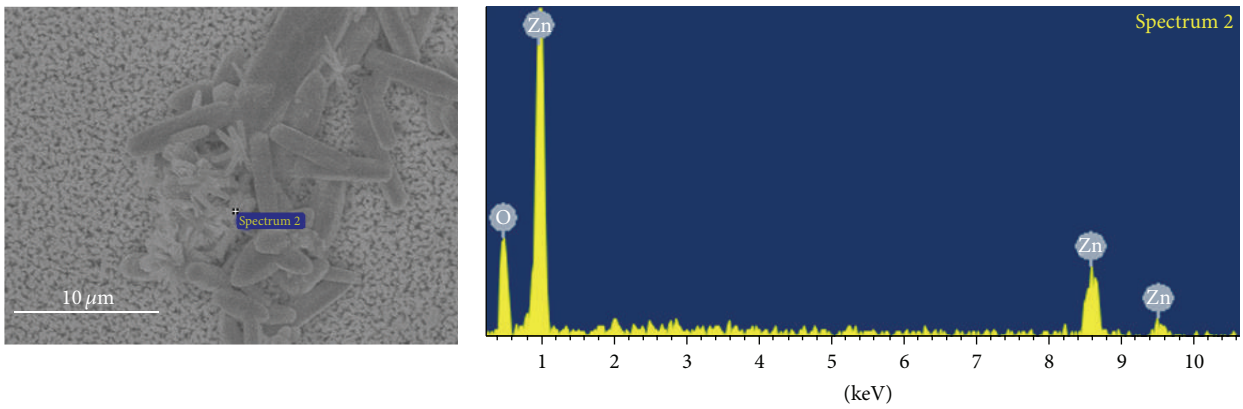

Figure 4: EDS analysis of the up-face ZnO films synthesized at 3 h.

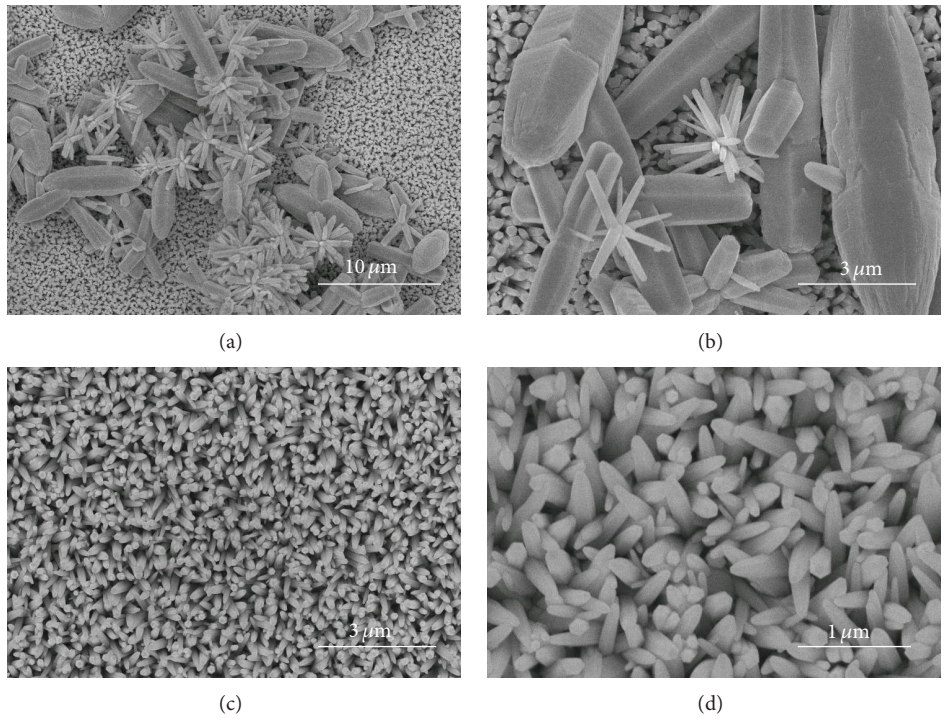

Figure 5: Surface morphologies of the ZnO films synthesized at different faces and different magnifications; the deposition time was 3 h. Up face with (a) lower magnification and (b) higher magnification; down face with (c) lower magnification and (d) higher magnification, respectively.

the results of XRD in Figure 3. The results in Figures 3 and 4 illustrate that the different lattice mismatches and defects affect the morphology as well as crystal orientation of the deposited ZnO films.

To investigate the general morphologies of as-synthesized ZnO nanorods and nanoflowers, the synthesized products are examined by FESEM and demonstrated in lower and higher magnification FESEM images, and the results are shown in Figure 5. The SEM images in Figures 5(a) and 5(b) clearly show that the up-face surfaces of the 3 h deposited $ZnO/SiO_2/Si$ substrates had been coated with non-uniform-sized ZnO nanorods, nanoflowers, and large hexagonal bars. The SEM images in Figures 5(c) and 5(d) clearly show that the down-face surfaces of the 3 h deposited $ZnO/SiO_2/Si$ substrates had been coated with uniform-sized and quasi-oriented ZnO nanorods. As we know, crystallization exists in two different successive stages: nucleation and crystal growth. The interaction between these two steps determines the crystal characteristics, including size, distribution, and morphology of the crystals. When the solutions are used to

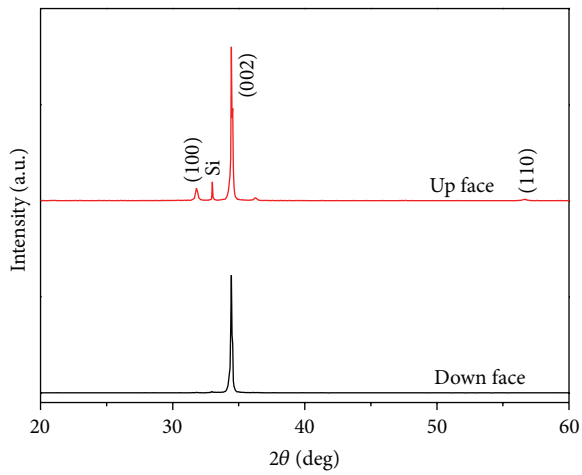

FIGURE 6: XRD patterns of the ZnO films synthesized at different faces; the deposition time was 3 h.

synthesize or deposit films, there are two different nucleation mechanisms in the solution: heterogeneous nucleation and homogenous nucleation [13]. Homogenous nucleation takes place when primary nucleation proceeds in a nucleation free solution; this is when the solution contains no foreign particles. Heterogeneous nucleation takes place if primary nucleation proceeds when foreign particles are present in the solution.

The reason for the different morphology of the synthesized ZnO films obtained on the two faces should be related to the different nucleation mechanisms in the solution. In our case, the growth of ZnO films on $ZnO/SiO_2/Si$ substrates at different faces was controlled by the two nucleation mechanisms. Li et al. have successfully grown large scale arrays of ZnO nanorods on zinc foil without the assistance of any template, oxidant, or coating of metal oxide layers, simply by dipping the foil into a 25% aqueous solution of ammonia (NH_4OH) and heating at a temperature 80°C in a Teflon-lined stainless steel autoclave [14]. They prepared four different samples by varying the concentration of ammonia in an 80 mL growth bath and the growth duration. They found that the thickness, density, and morphology of the ZnO nanorods are affected by the alkalinity of the solution in the growth bath. However, in this study we prove that with the addition of ZnO films as seed layer on SiO_2/Si substrates we can synthesize the nanorods and nanoflowers at 100°C. Those results also suggest that we can control the number of the irregular-plate type ZnO, ZnO nanorods, and ZnO nanoflowers on $2 \times 2\,cm^2$ sample by controlling the deposition time and direction (down face or up face) of $ZnO/SiO_2/Si$ substrates.

Figure 6 shows the XRD spectra of the 3 h deposited ZnO films prepared at different faces. Results indicate that down-face ZnO films only had a strong (002) peak and up-face ZnO films had a strong (002) peak and two weak (100) and (110) peaks preferred orientation with the *c*-axis perpendicular to the substrate. All the (002) peaks in Figure 6 were found at $2\theta \sim 34.45^\circ$, which was the same as the stoichiometric ZnO crystal ($2\theta \sim 34.45^\circ$). These results imply that the parameter of lattice constant *c* is unchanged as different faces of $ZnO/SiO_2/Si$ substrates are used in the synthesizing process. The results for XRD patterns of the ZnO films in Figures 4 and 6 can be described as a number of alternating planes composed of tetrahedrally coordinated O^{2-} and Zn^{2+} stacked alternately along the *c*-axis. Also, the ZnO films exhibit a varied range of novel structures. These structures can be grown by tuning the growth rates along different fast growing directions. As those results in SEM images and XRD patterns, changing the face of the $ZnO/SiO_2/Si$ substrates will change the nucleation mechanisms and then change the synthesizing results of the ZnO films, because homogenous nucleation produces undesired ZnO particles and heterogeneous nucleation produces nanorods. As the ZnO seed layer is grown on the SiO_2/Si substrates, we think the irregular-plate type ZnO is grown under the heterogeneous nucleation, which is much more common than homogeneous nucleation. Heterogeneous nucleation is typically much faster than homogeneous nucleation because the nucleation barrier (ΔG^*) is much lower at a surface. For that, the irregular-plate type ZnO is grown first. However, ZnO nanorods are limited by homogenous nucleation of ZnO particles that align the *c*-axis and ZnO nanoflowers are homogenous nucleation in a different crystalline direction as the nanorods are grown too long.

4. Conclusions

As the synthesized time was 1 h, 3 h, and 5 h, the down-face morphologies of ZnO films on $ZnO/SiO_2/Si$ substrates were irregular-plate structure films, ZnO nanorods with a diameter ranging from 65 to 200 nm, and beautiful chrysanthemum- (flower-) like clusters grown above the nanorods in very large quantity, respectively. As the synthesized time was 1 h, 3 h, and 5 h, the pure ZnO nanorods could not be obtained in up-face ZnO films. XRD patterns indicated that 1 h and 5 h deposited ZnO films had a (002) peak and two weak (100) and (110) peaks and 3 h deposited ZnO films only had a strong (002) peak. The reason for different morphologies of the ZnO films obtained on the two faces should be related to the two nucleation mechanisms, heterogeneous nucleation and homogenous nucleation, in the solution. As deposition time was 3 h, the down-face morphology of ZnO films was only ZnO nanorods with a diameter ranging from 65 to 200 nm and in very large quantity, which could be investigated as gas sensors.

Conflict of Interests

The authors have no financial competing interests.

Acknowledgments

The authors acknowledge financial supports of NSC 102-2221-E-218-036, NSC 102-2622-E-390-002-CC3, and NSC 102-2221-E-390-027.

References

[1] F. H. Wang, C. F. Yang, and Y. H. Lee, "Deposition of F-doped ZnO transparent thin films using ZnF_2-doped ZnO target under different sputtering substrate temperatures," *Nanoscale Research Letters*, vol. 9, article 97, 2014.

[2] J. Chung, J. Lee, and S. Lim, "Annealing effects of ZnO nanorods on dye-sensitized solar cell efficiency," *Physica B*, vol. 405, no. 11, pp. 2593–2598, 2010.

[3] N. Saito, H. Haneda, T. Sekiguchi, N. Ohashi, I. Sakaguchi, and K. Koumoto, "Low-temperature fabrication of light-emitting zinc oxide micropatterns using self-assembled monolayers," *Advanced Materials*, vol. 14, no. 6, pp. 418–421, 2002.

[4] G. Kwak, M. Seol, Y. Tak, and K. Yong, "Superhydrophobic znO nanowire surface: chemical modification and effects of UV irradiation," *Journal of Physical Chemistry C*, vol. 113, no. 28, pp. 12085–12089, 2009.

[5] L. Wang, Y. Kang, X. Liu, S. Zhang, W. Huang, and S. Wang, "ZnO nanorod gas sensor for ethanol detection," *Sensors and Actuators, B: Chemical*, vol. 162, no. 1, pp. 237–243, 2012.

[6] L. Li, H. Yang, H. Zhao et al., "Hydrothermal synthesis and gas sensing properties of single-crystalline ultralong ZnO nanowires," *Applied Physics A*, vol. 98, no. 3, pp. 635–641, 2010.

[7] J. Kim and K. Yong, "Mechanism study of ZnO nanorod-bundle sensors for H_2S gas sensing," *Journal of Physical Chemistry C*, vol. 115, no. 15, pp. 7218–7224, 2011.

[8] H. Ghayour, H. R. Rezaie, S. Mirdamadi, and A. A. Nourbakhsh, "The effect of seed layer thickness on alignment and morphology of ZnO nanorods," *Vacuum*, vol. 86, no. 1, pp. 101–105, 2011.

[9] X. Jiaqiang, C. Yuping, C. Daoyong, and S. Jianian, "Hydrothermal synthesis and gas sensing characters of ZnO nanorods," *Sensors and Actuators, B: Chemical*, vol. 113, no. 1, pp. 526–531, 2006.

[10] L. Vayssieres, "Growth of arrayed nanorods and nanowires of ZnO from aqueous solutions," *Advanced Materials*, vol. 15, no. 5, pp. 464–466, 2003.

[11] G. Kenanakis, D. Vernardou, E. Koudoumas, and N. Katsarakis, "Growth of c-axis oriented ZnO nanowires from aqueous solution: The decisive role of a seed layer for controlling the wires' diameter," *Journal of Crystal Growth*, vol. 311, no. 23-24, pp. 4799–4804, 2009.

[12] X. Liu, Z. Jin, S. Bu, J. Zhao, and Z. Liu, "Effect of buffer layer on solution deposited ZnO films," *Materials Letters*, vol. 59, no. 29-30, pp. 3994–3999, 2005.

[13] V. L. Snoeyink and D. Jenkins, *Water Chemistry*, John Wiley & Sons, 1980.

[14] Z. Li, X. Huang, J. Liu, Y. Li, X. Ji, and G. Li, "Growth and comparison of different morphologic ZnO nanorod arrays by a simple aqueous solution route," *Materials Letters*, vol. 61, no. 22, pp. 4362–4365, 2007.